Title	Development of a multiphysics model to characterize the responsive behavior of urea-sensitive hydrogel as biosensor
Author(s)	Goh, K. B.; Li, Hua; Lam, Khin Yong
Citation	Goh, K. B., Li, H., & Lam, K. Y. (2017). Development of a multiphysics model to characterize the responsive behavior of urea-sensitive hydrogel as biosensor. Biosensors and Bioelectronics, 91, 673-679.
Date	2017
URL	http://hdl.handle.net/10220/42498
Rights	© 2017 Elsevier B. V. This is the author created version of a work that has been peer reviewed and accepted for publication by Biosensors and Bioelectronics, Elsevier. It incorporates referee's comments but changes resulting from the publishing process, such as copyediting, structural formatting, may not be reflected in this document. The published version is available at: [http://dx.doi.org/10.1016/j.bios.2017.01.023].

Development of a multiphysics model to characterize the responsive behavior of urea-sensitive hydrogel as biosensor

K.B. Goh, Hua Li [*], K.Y. Lam

School of Mechanical and Aerospace Engineering, Nanyang Technological University, Nanyang Avenue, Singapore 639798, Republic of Singapore

Abstract: A remarkable feature of biomaterials is their ability to deform in response to certain external bio-stimuli. Here, a novel biochemo-electro-mechanical model is developed for the numerical characterization of the urea-sensitive hydrogel in response to the external stimulus of urea. The urea sensitivity of the hydrogel is usually characterized by the states of ionization and denaturation of the immobilized urease, as such the model includes the effect of the fixed charge groups and temperature coupled with pH on the activity of the urease. Therefore, a novel rate of reaction equation is proposed to characterize the hydrolysis of urea that accounts for both the ionization and denaturation states of the urease subject to the environmental conditions. After examination with the published experimental data, it is thus confirmed that the model can characterize well the responsive behavior of the urea-sensitive hydrogel subject to the urea stimulus, including the distribution patterns of the electrical potential and pH of the hydrogel. The results point to an innovative means for generating electrical power via the enzyme-induced pH and electrical potential gradients, when the hydrogel comes in contact with the urea-rich solution, such as human urine.

---

[*] Corresponding author, Tel.: + 65 6790 4953; Fax: + 65 6792 4062
Email address: lihua@ntu.edu.sg (Hua Li)

1. Introduction

According to Mayo clinic the chronic kidney disease (CKD) is characterized by the gradual loss of kidney functions over time (Ficalora, 2013). As the CKD progresses to the advanced-stage, a dangerous level of urea and electrolytes build-up in the human system, which increases the risk of cardiovascular, hyperlipidemia, anemia and metabolic bone diseases (Thomas et al., 2008). Therefore, the urea and electrolytes levels in the human blood and urine are measured for CKD patients during medical evaluation, since it provides access to the state of health of the kidney. As such, there were great attempt to develop the urea biosensors to estimate the blood urea nitrogen (BUN) levels for CKD patients by means of integrating urease into the hydrogel (Dezhong et al., 1996; Kovács et al., 2003; Liu et al., 1996). However, it is evident from the open literature that the performance of the hydrogel in response to the external stimulus of urea is still poorly understood. Therefore, in this paper, a multiphysics model is developed to investigate the responsive behavior of the hydrogel subject to the external stimulus of urea at different environmental conditions.

It is found in the open literature that the urea-sensitive hydrogel-based biosensors were synthesized using the pH- or temperature-sensitive hydrogels, i.e. poly(vinyl alcohol) (Jha et al., 2008; Marchenko et al., 2015), polyaniline (Buron et al., 2014), poly(o-phenylenediamine) (Chirizzi and Malitesta, 2011), poly(carbamoylsulfonate) (Eggenstein et al., 1999), and poly(3-cyclohexyl thiophene) (Pandey et al., 2000). Moreover, most researchers opted for gamma radiation (Hamdy et al., 2008), covalent binding (Chen and Chiu, 1999, 2000; Chen et al., 1994; Miyata et al., 1997), or physical entrapment (Hamilton and Breslin, 2014) for the amalgamation of the urease with the polymer network chains for the synthesis of the urea-sensitive hydrogel.

2

As such, it is reported that the integration of the urease with the polymer network chains improved the mechanical properties of the hydrogel and stability of the urease, which may then prolong the life shelf of the biosensors (Novick and Dordick, 1998; Teixeira et al., 2012).

As mentioned above, despite the extensive experimental investigations carried out on the urea-sensitive hydrogel, very few efforts were made via theoretical modeling and numerical simulation for the examination of the hydrogels. From the open literature, it is found that most of the published mathematical models were unable to capture the coupled biochemo-electro-mechanical behavior of the hydrogel. For example, the published mathematical models were inadequate in predicting the volumetric behavior of the hydrogels in response to the urea, where the simulated diffusion and reaction of the reactive solutes were associated with the urea hydrolysis and not the concomitant mechanical behavior of the hydrogels (Blaedel and Kissel, 1975; Chen and Chiu, 2000), including Moynihan et al. (1989) and Chowdhury and Bhattacharya (1997), where they modelled the kinetic parameters of the urea-sensitive hydrogel via the mass balance and Michaelis-Menten equations.

It is known that the mathematical correlation presented by Ogawa and Kokufuta may be the first work to attempt to predict the mechanical deformation of the hydrogels in response to urea (Ogawa and Kokufuta, 2002). The mathematical correlation was obtained from the experimental pH-responsive equilibrium swelling of the hydrogel, where the correlation was limited to the swelling at pH 4~7 immersed in 5 mM maleate-buffer solution of $35\,^{\circ}\text{C}$. Therefore, the correlation was unable to estimate the equilibrium swelling ratio of the hydrogel at different environmental conditions other than the prescribed conditions. It is also noted that the influence of environmental pH on the activity of the urease was accounted for in their reaction-diffusion

3

model, while the effect of pH coupled with temperature on the performance of the urease was excluded. Moreover, the effect of the fixed charge groups in the hydrogels was also neglected by all the published models mentioned above on the distribution pattern of the concentration of the reactive mobile ions. In order to overcome these limitations of the published mathematical models, a multi-effect-coupling urea-stimulus (MECurea) model is proposed in this paper to investigate the performance of the hydrogels in response to urea.

2. Formulation of the MECurea model

In order to formulate the model, a few components are prescribed delicately, given as follows: (a) the movement of mobile solutes between the hydrogel and surrounding solution; (b) the enzymatic hydrolysis reaction of urea within the hydrogel; (c) the interaction between the mobile ions and fixed charge in the hydrogel; (d) the swelling forces arising from the biochemical reactions and (f) the swelling behavior of the hydrogels, as illustrated in Fig. 1.

The present MECurea model is formulated based on the following assumptions:

(i) The hydrogel is maintained at the isothermal condition, such that the rate of reaction r_k is constant.

(ii) The urease is immobilized and distributed uniformly within the hydrogel, where the activity of the urease is also constant.

(iii) The optimum temperature T_{op} of urease is equal to the temperature at the midpoint of transition between active and inactive forms T_{eq}, such that $\Delta H_{eq} \approx 2\Delta G_{cat}$, where ΔH_{eq} is the enthalpy change associated with the conversion of an active to an inactive enzyme, and ΔG_{cat} is the activation energy of the catalytic reaction (Peterson et al., 2004).

4

(iv) The hydrogel has a macroporous nature such that the diffusivity coefficients D_k of the mobile solutes are the same in both the hydrogels and surrounding solution.

(v) The solution flow is very slow and the convection term is neglectable, where the urea hydrolysis in the dilute buffer solution is also neglected.

2.1 Conservation of mass

In the MECurea model, at least six mobile ions and one molecule are considered in the present system, namely the hydrogen ion (H$^+$), hydroxide ion (OH$^-$), ammonium ion (NH$^+_4$), bicarbonate ion (HCO$^-_3$), cation and anion species, and urea. The Nernst-Planck equation is used to characterize the fluxes of the mobile solutes, given as follows (Li et al., 2009)

$$\nabla \cdot \left(\mathbf{C}^{-1} D_k \left[\nabla C_k + \frac{z_k F}{RT} C_k \nabla \Phi \right] \right) = v_k r_k \left(k = H^+, OH^-, ..., N \right) \tag{1}$$

where $\mathbf{C}^{-1}$ the inverse of the right Cauchy-Green tensor and $\mathbf{C}^{-1} = \mathbf{F}^{-1}\mathbf{F}^{-T}$. D_k, C_k, z_k, v_k and r_k indicate the diffusivity tensor (m^2/s), concentration (mM), valence number, stoichiometric coefficient in the chemical reaction, and rate of chemical reaction for the kth mobile species. $R, T, F,$ and Φ denote the universal gas constant (8.314 J/mol K), absolute temperature (K), Faraday constant (96487 C/mol), and electrostatic potential of the hydrogel. For the non-ionic solute where the charge $z_k = 0$, the Nernst-Planck Eq. (1) is reduced to Fick's first law of diffusion.

2.2 Conservation of momentum

The bioelectrochemistry reaction within the hydrogel gives rise to the swelling pressure, resulting in the configurational changes or swelling deformation of the urea-sensitive hydrogel. It is known that the swelling of the hydrogel progresses, until the swelling forces are balanced by

5

the restrictive forces exerted by the elastic structure of the polymer network chains to achieve the equilibrium hydration state. In order to formulate this phenomenon, the law of conservation of linear momentum is employed, given as follows

$$\nabla \cdot \mathbf{P} = \mathbf{0} \tag{2}$$

where $\mathbf{P}$ is the Piola stress.

2.3   Free energy imbalance inequality for constitutive equation

In order to develop the equations of state for the hydrogel subject to the isothermal condition, the local free energy imbalance inequality is written as follows (Drozdov and deClaville Christiansen, 2015c)

$$\dot{W} - \left(u_1 + u_2 + u_3 \right) \le 0 \tag{3}$$

where $\dot{W}$ is temporal increase of the Helmholtz free energy density of the hydrogel, while u_1, u_2 and u_3 denote the rate of work per volume expanded into the system by the mechanical, electric and chemical fields.

The free energy density of an idealized ionic hydrogel is defined as a sum of four components (Drozdov and deClaville Christiansen, 2015b): (i) the free energy density of stretching of the polymer network chains W_1, (ii) the free energy density of mixing the polymer and solvent W_2, (iii) the free energy density due to entropy mixing of mobile ions and solvent W_3, and (iv) the free energy density of the electric field formed by mobile ions and bound charges W_4

$$W = W_1 + W_2 + W_3 + W_4 \tag{4}$$

The free energy density of elastic stretching of the polymer network chains is given as (Hong et al., 2008)

6

$$W_1 = \frac{1}{2} Nk_B T \left[\mathrm{tr}\left(\mathbf{F}^T \mathbf{F}\right) - 2\ln\left(\det \mathbf{F}\right) - 3 \right] \tag{5}$$

where $Nk_B T$ is the ground-state shear modulus G, N is the number of polymer chains per volume of the dry polymer ($2.43 \times 10^{-23}\,\mathrm{m}^{-3}$), and k_B is the Boltzmann constant (1.381×10^{-23} J/ K). Based on the theory of multiplicative decomposition of the deformation gradient (Chester, 2015), the right Cauchy-Green tensor is written as $\mathbf{C} = \left(\lambda_s\right)^2 \mathbf{C}_e$, where λ_s is the swelling stretch and $\mathbf{C}_e$ is the elastic right Cauchy-Green tensor. As such, W_1 is recast to

$$W_1 = \frac{1}{2} Nk_B T \left[\left(\lambda_s\right)^2 \mathrm{tr}\left(\mathbf{C}_e\right) - 2\ln\left(\det \mathbf{F}\right) - 3 \right] \tag{6}$$

The free energy density of mixing between the polymer and solvent is taken as (Chester, 2015; Drozdov and deClaville Christiansen, 2015a)

$$W_2 = RTC\left(\ln\left(C\upsilon\right) - \ln\left(1 + C\upsilon\right) + \frac{\chi}{1 + C\upsilon} \right) \tag{7}$$

where C is the concentration of the solvent, υ is the volume of a mole of fluid molecules and χ is the Flory-Huggins interaction parameter.

The free energy density due to the entropy of mixing free energy of the solvent and mobile ions is given as (Doi, 2013)

$$W_3 = RT \sum_k C_k \left(\ln C_k - \ln C - 1 \right) \tag{8}$$

The free energy density of the electric field formed by the mobile ions and fixed charge groups is given as follows (Hong et al., 2008)

$$W_4 = \frac{1}{2\varepsilon_r \varepsilon_0 J} \left(\mathbf{H} \cdot \mathbf{C} . \mathbf{H} \right) \tag{9}$$

7

where $J = \left(\lambda_s\right)^3$, $\mathbf{H}$ is the dielectric displacement, and $\varepsilon_r \varepsilon_0$ is the relative dielectric constant. It is understood that the volume change of the hydrogel is due to swelling and W_4 is rewritten as follows (Chester, 2015)

$$W_4 = \frac{1}{2\varepsilon_r \varepsilon_0 \left(1 + C\upsilon\right)^{1/3}} \left(\mathbf{H} \cdot \mathbf{C}_e \cdot \mathbf{H}\right) \tag{10}$$

The mechanical power per volume is given by (Belytschko et al., 2013; Gurtin et al., 2010)

$$u_1 = J\sigma : \mathbf{L} \tag{11}$$

where σ is the symmetric Cauchy stress tensor and $\mathbf{L}$ is the velocity u_1 is given as (Chester, 2015; Gurtin et al., 2010)

$$u_1 = \left(\mathbf{P}\mathbf{F}_s^T + Jp\mathbf{F}_e^{-T}\right) : \dot{\mathbf{F}}_e - \dot{J}_s p \tag{12}$$

where $\mathbf{F}_s$ is the deformation gradient for the swelling of the hydrogel, while $\mathbf{F}_e$ is the deformation gradient for the elastic deformation of the hydrogel.

The rate of work done by electric field per volume is written as follows (Drozdov and deClaville Christiansen, 2015c)

$$u_2 = \mathbf{E} \cdot \dot{\mathbf{H}} - F\Phi \sum_k z_k \dot{C}_k \tag{13}$$

The last power term is produced due to the transport of solvent and mobile ions per volume given as (Nardinocchi et al., 2011)

$$u_3 = -\left(\mu \nabla \cdot \mathbf{J} + \sum_k \mu_k \nabla \cdot \mathbf{J_k}\right) - \left(\mathbf{J}\nabla\mu + \sum_k \mathbf{J}_k \nabla\mu_k\right) \tag{14}$$

where μ and μ_k are the chemical potentials of solvent and mobile ion k and $\mathbf{J}$ and $\mathbf{J}_k$ are the fluxes of solvent and mobile ion k. The free energy imbalance inequality equation for characterizing the responsive behavior of the urea-sensitive hydrogels is given as follows

8

$$\frac{1}{(1+C\upsilon)^{1/3}}\left(Nk_BT\left(1+C\upsilon\right) \mathbf{F}_e + \frac{1}{\varepsilon}\left(\mathbf{F}_e\left(\mathbf{H}\otimes\mathbf{H}\right)\right) - \left(1+C\upsilon\right)^{4/3}\left(\sigma\,\mathbf{F}_e^{-T} + p\,\mathbf{F}_e^{-T}\right)\right):\dot{\mathbf{F}}_e$$

$$+\dot{C}\left(\mu + Nk_BT\left[\frac{\upsilon}{(1+C\upsilon)^{1/3}}\left(\frac{1}{3}\mathrm{tr}(\mathbf{C}_e) - \frac{1}{(1+C\upsilon)^{2/3}}\right)\right] + RT\left(\ln\frac{C\upsilon}{1+C\upsilon} + \frac{1}{1+C\upsilon} + \frac{\chi}{(1+C\upsilon)^2}\right)\right) \quad (15)$$

$$-\dot{C}\left(-p\upsilon + RT\sum_k\left(\frac{C_k}{C}\right) + \frac{1}{6\varepsilon_r\varepsilon_0}\frac{\upsilon}{(1+C\upsilon)^{4/3}}\left(\mathbf{H}\cdot\mathbf{C}_e\cdot\mathbf{H}\right)\right) + \dot{C}_k\left(RT\ln\frac{C_k}{C} + z_kF\Phi - \mu_k\right)$$

$$+\left(\mathbf{J}\nabla\mu + \sum_k\mathbf{J}_k\nabla\mu_k\right)\leq 0$$

2.4 Biochemistry for constitutive equation

To implement Eq. (1), the classical rate of chemical reaction r_k that characterizes the reaction of urea in the present of urease is given as follows (Fogler, 2010)

$$r_k = k_{cat}\frac{C_{E_{act}}C_{urea}}{K_M} \quad (16)$$

where $C_{E_{act}}$ and C_{urea} are the concentrations of the active enzyme and urea, respectively. k_{cat} is the constant catalytic rate of the enzyme and K_M is the Michaelis constant. It is found that Eq. (16) excludes the effect of urease denaturation. As such, in the present of denaturation of urease due to temperature, Eq. (16) is rewritten as (Peterson et al., 2007)

$$r_k = V_{max}\,C_{urea}\frac{1+K_{EQ}}{C_{urea} + K_M K_{EQ}} \quad (17)$$

where V_{max} is the maximum velocity that can be achieved by a given quantity of an enzyme, and

$V_{max} = \dfrac{k_{cat}C_{E_{act}}}{1+K_{EQ}}$ (Menichetti et al., 2015), $K_{EQ} = \exp\left[\dfrac{\Delta H_{eq}}{R}\left(\dfrac{1}{T_{eq}} - \dfrac{1}{T}\right)\right]$ is the equilibrium

constant between active and inactive urease, and C_{E_0} is the initial concentration of the urease in the system.

9

The denaturation of urease due to pH is characterized by (Tijskens et al., 2001)

$$\text{(a)} \quad C_{E_{act}} + C_{OH^-} \overset{K_{EOH}}{\Leftrightarrow} C_{EOH^-_{inact}} \overset{k_{inact}}{\to} C_X \tag{18}$$

$$\text{(b)} \quad C_{E_{act}} + C_{H^+} \overset{K_{EH}}{\Leftrightarrow} C_{EH^+_{inact}} \overset{k_{inact}}{\to} C_X \tag{19}$$

where $C_{EH^+_{inact}}$ and $C_{EOH^-_{inact}}$ are the concentration of the protonated and hydroxylated ureases, which are completely inactive but not denature, and C_X is the concentration of the denatured urease (Fidaleo and Lavecchia, 2003; Tijskens et al., 2001). K_{EOH} and K_{EH} are the equilibrium constant for the hydroxylation and protonation of the urease, and K_W is the water dissociation constant. As such, the concentration difference of total and denatured enzymes is given as

$$C_{E_0} - C_X = C_{E_{act}} \left(1 + \frac{K_W}{K_{EOH} C_{H^+}} + \frac{C_{H^+}}{K_{EH}} \right) \tag{20}$$

Finally, the rate of chemical reaction r_k is further recast for the effect of temperature coupled with pH on the activity of the urease into the following

$$r_k = V_{\max} \frac{C_{urea}}{K_M} \left(\frac{C_{urea}}{K_M} + K_{EQ} \right) \left(1 + \frac{K_{EOH} C_{H^+}}{K_W} + \frac{K_{EH}}{C_{H^+}} \right) \tag{21}$$

2.5 Electrical field for constitutive equation

In order to consider the coupled effect of the electrical potential Φ of the hydrogel and the movement of ionic solutes k, the Poisson equation is incorporated into the MECurea model by (Li et al., 2009)

$$\nabla \cdot \left(\varepsilon_r \varepsilon_0 \, J \, \mathbf{C}^{-1} \nabla \Phi \right) = -F \left(\sum_k z_k C_k + z_f C_f \right) \tag{22}$$

10

where fixed charge concentration C_f of an anionic hydrogel is given as (Grimshaw et al., 1990)

$$C_f = \frac{C_f^0}{H} \frac{K}{K + C_{H^+}}$$

(23)

where C_f^0 is the initial fixed charge concentration at the hydrogel dry state, H is the ratio of final to the initial volume of the hydrogel, and K is the dissociation constant of the fixed charge groups.

2.6 Mechanical field for constitutive equation

From Eq. (15), when the system is in mechanical equilibrium the term in the first bracket vanishes and the Piola stress $\mathbf{P}$ is given as follows (Hong et al., 2008)

$$\mathbf{P} = -(1 + C\upsilon)^{2/3} p \mathbf{F}_e^{-T} + N k_B T (1 + C\upsilon)^{1/3} \mathbf{F}_e + (1 + C\upsilon)^{-2/3} \mathbf{F}_e \frac{1}{\varepsilon} (\mathbf{H} \otimes \mathbf{H})$$

(24)

where the Piola stress $\mathbf{P}$ is balanced by the osmotic pressure p, elastic polymeric network chains stress, and Maxwell stress. At the equilibrium state, the Maxwell stress is neglectable (Drozdov and deClaville Christiansen, 2015c), such that the Piola stress $\mathbf{P}$ is reduced to

$$\mathbf{P} = -(\lambda_s)^2 p \mathbf{F}_e^{-T} + N k_B T (\lambda_s) \mathbf{F}_e$$

(25)

Again from Eq. (15), when the system is at steady-state, the chemical potentials of the interior and exterior solutions are given as follows (Illeperuma et al., 2013)

$$\mu = RT \frac{\sum_k C_k}{C} - RT \left(\ln \frac{C\upsilon}{(1 + C\upsilon)} - \frac{1}{(1 + C\upsilon)} + \frac{\chi}{(1 + C\upsilon)^2} \right)$$
$$- N k_B T \left[\frac{\upsilon}{(1 + C\upsilon)^{1/3}} \left(\frac{1}{3} \mathrm{tr}(\mathbf{C}_e) - \frac{1}{(1 + C\upsilon)^{2/3}} \right) \right] - \upsilon p$$

(26)

$$\bar{\mu} = RT \frac{\sum_k \overline{C}_k}{\overline{C}}$$

(27)

11

where the overbar indicates the parameters in the surrounding solution.

By adopting the Donnan equilibrium, where the chemical potentials in the interior and exterior solutions coincide over the hydrogel-solution interface, namely $\mu = \overline{\mu}$, the osmotic pressure p is given as (Drozdov and deClaville Christiansen, 2015b)

$$
\begin{aligned}
p = RT \sum_k \left(\frac{C_k}{J-1} - \overline{C}_k \right) - \frac{RT}{\upsilon} \left(\ln \frac{C\upsilon}{(1+C\upsilon)} - \frac{1}{(1+C\upsilon)} + \frac{\chi}{(1+C\upsilon)^2} \right) \\
- Nk_B T \left[\frac{1}{(1+C\upsilon)^{1/3}} \left(\frac{1}{3} \operatorname{tr}(\mathbf{C}_e) - \frac{1}{(1+C\upsilon)^{2/3}} \right) \right]
\end{aligned}
\tag{28}
$$

where the first term on the right-hand side arises due to the imbalance distribution of ionic concentrations between the hydrogel and surrounding solution, the second term is due to the mixing of the solvent and hydrogel, and the third term is due to the elastic stretching of the polymeric network chains. It is noted that the osmotic pressure p here is consistent with the published results in the open literature (Duda et al., 2010; Marcombe et al., 2010).

2.7   Boundary conditions

In this section, to investigate the responsive behavior of the cylindrical-shaped urea-sensitive hydrogel immersed in the flow of urea-buffer solution, one-dimensional steady-state numerical simulations of the MECurea model are conducted. The hydrogel is taken as symmetrical and has a large length/radial ratio property, where the deformation of the urea-sensitive hydrogel is taken at the radial direction and restricted in the axial direction, such that the deformation of the hydrogel is a one-dimensional problem. (Deen, 1998). The computation domain includes both the hydrogel and buffer solution, while the momentum Eq. (2) only covers the hydrogel domain.

The Neumann type boundary conditions are imposed at the center of the cylindrical hydrogel to ensure the continuity in the hydrogel, given as follows

$$\frac{\partial C_k}{\partial X} = 0, \ \frac{\partial \Phi}{\partial X} = 0 \left(k = H^+, OH^-, ..., N \right) \text{ at } X = 0 \tag{29}$$

while the Dirichlet boundary conditions along the solution

$$C_k = \overline{C}_k, \ \Phi = 0 \left(k = H^+, OH^-, ..., N \right) \tag{30}$$

In order to consolidate the mechanical equilibrium equation with Eq. (2), Eq. (25) is further elaborated to the following form

$$\mathbf{P} = -\left(\lambda_s \right)^2 p(1) + N k_B T (\lambda_s) \left(1 + \frac{\partial u_e}{\partial X} \right) \tag{31}$$

where the radial swelling stretch λ_s is given as

$$\lambda_s = \frac{\partial x_s}{\partial X} = 1 + \frac{\partial u_s}{\partial X} = \frac{L_{gel}}{L^o_{gel}} \tag{32}$$

where u_s is the swelling displacement and L_{gel} is the diameter of the gel.

By Eq. (31), the Piola stress $\mathbf{P}$ is further rewritten as follows

$$\mathbf{P} = -\left(1 + \frac{\partial u_s}{\partial X} \right)^2 p(1) + N k_B T \left(1 + \frac{\partial u_s}{\partial X} \right) \tag{33}$$

and by substituting Eq. (33) into the momentum Eq. (2) we obtain

$$\frac{\partial}{\partial X} \left[-\left(1 + \frac{\partial u_s}{\partial X} \right)^2 p + N k_B T \left(1 + \frac{\partial u_s}{\partial X} \right) \right] = 0 \tag{34}$$

Finally, the swelling stretch λ_s between the hydrogel-solution interfaces is expressed as

$$\lambda_s = \frac{N k_B T}{p}, \ \ X = L_{gel} \tag{35}$$

In order to simulate the responsive behavior of the hydrogel, the commercial finite-element solver, COMSOL Multiphysics 5.1 is employed for the numerical solution of the MECurea model due to the ability in efficiently handling the coupled governing equations with desired

computational accuracy. As such, the fixed charge density Eq. (23) is first solved to obtain the concentration of the fixed charge C_f according to the given boundary conditions and input parameter. By the computed C_f, the Nernst-Planck equation Eq. (1) coupled with the Poisson equation Eq. (22) are solved numerically for the converged solution of mobile species concentration C_k and electric potential Φ. The converged solution of mobile species concentration C_k is then employed into the nonlinear mechanical equilibrium equation Eq. (35) for the corresponding swelling stretch λ_S. Lastly, the stretching of the hydrogel causes the redistribution of the mobile ions and fixed charge groups within the hydrogel, such that a new iteration is started until all the independent variables reach convergence, including C_k, Φ, C_f and λ_S.

3. Result and discussions

3.1 Validation of the MECurea model

To validate the MECurea model, the equilibrium swelling behavior of urea-sensitive hydrogels is examined by comparing the present numerical result with the experimental data, as shown in Fig. 2, in which a good agreement is achieved. In the experimental work conducted by Ogawa and Kokufuta (Ogawa and Kokufuta, 2002), the urea-sensitive p(NIPAM)-based hydrogels with diameter of 290 μm was immersed in the flow of maleate-buffer of 5 mM, containing the urea of $\overline{C}_{urea}$=1 mM, with pH = 4, at the temperature of 35 $^{\text{o}}$C, such that the urease concentration C_{E_0} of 0.2 to 8.0 mg/mL immobilized in the hydrogel. Several input are required by the MECurea model for the numerical simulation of the hydrogel, such as $L = 2500$ μm, $z_k = -1$, C_f^0=0.775 mmol/g, $K = 10^{-5.57}$, while the remaining inputs are given in Table 1.

14

Fig. 2 indicates that the hydrogel swells drastically less at a higher concentration of immobilized urease C_{E_0} (i.e. more than 0.5 mg/mL), such that the entrapped urease improves the mechanical properties of the polymeric network chains, resulting in a stronger hydrogel and limit the swelling of the urea-sensitive hydrogel. For the hydrogels with a smaller concentration of the immobilized urease C_{E_0} (i.e. less than 0.5 mg/mL), the present numerical results usually overestimate the experimental equilibrium swelling behavior as compared to the published numerical results, however the errors of the present numerical simulations are usually within the experimental error of $\pm 13\ \mu m$, as seen in Fig. 2. Based on the comparison in Fig. 2, it is concluded that the numerical result of the MECurea model agrees well with the experimental findings.

3.2 The performance of the hydrogel in response to the urea cue

A case study through the numerical simulation of the MECurea model is conducted for the response of the anionic urea-sensitive hydrogel with $z_f = -1$ subject to the urea at different environmental temperatures. The material properties required by the MECurea model are given as $L = 250\ \mu m$, $L_{gel}^0 = 50\ \mu m$, $C_f^0 = 1800$ mM, $K = 10^{-2.0}$, and the other input parameters are tabulated in Table 1. For the present simulation, the hydrogel is immersed in the phosphate-buffered saline (PBS) solution ($\overline{C}_{Na^+} = 142$ mM and $\overline{C}_{Cl^-} = 103$ mM), where the urea concentration $\overline{C}_{urea}$ ranging from 0 to 2000 mM at pH=7.40 is taken as the input with the solution temperature of 34 ~ 40 °C with 0.5 mg/mL urease concentration C_{E_0} immobilized in the hydrogel.

15

Fig. 3 is plotted to illustrate the responsive deformation of the urea-sensitive hydrogel subject to the change of urea concentration $\overline{C}_{urea}$ in the buffer solution at different environmental temperatures. It is found that the hydrogel collapses with the increase of the urea concentration $\overline{C}_{urea}$, where the hydrogel further collapses with the increase of the surrounding temperature. Furthermore, the responsive behavior of the hydrogel is divided into three stages, as shown in Fig. 3: (1) the hydrogel shows no noticeable change of swelling ratio with the increment of the environmental urea concentration $\overline{C}_{urea}$ smaller than 1 mM, (2) the hydrogel starts to collapse, when the environmental urea concentration $\overline{C}_{urea}$ is larger than 1 mM, and (3) the hydrogel begins to swell again, when the environmental urea concentration $\overline{C}_{urea}$ is larger than 400 mM. As such, the mechanical sensitivity of the hydrogel falls in the range of urea concentration $\overline{C}_{urea}$ 1 to 100 mM, since the hydrogel collapses drastically at this range of urea concentration $\overline{C}_{urea}$, as shown in Fig. 3.

Fig. 4 is plotted to visualize the distributive electrical potential within the hydrogel and surrounding solution subject to different concentrations of urea $\overline{C}_{urea}$. At $\overline{C}_{urea} = 100$ and 200 mM, where the fixed charge groups are mainly ionized, a constant electrical potential is found within the hydrogel, while the electrical potential Φ is equal to zero in the external solution since there is electroneutrality state in the total concentrations of all the mobile ionic solutes. To our best knowledge, this is the first example of biomaterial which exhibits the electrical potential gradient in response to the urea cue above 1000 mM, as shown in Fig. 4.

Fig. 5 illustrates the distribution profile of the pH in both the hydrogel and surrounding solution, when immersed in the urea-buffer solution of $\overline{C}_{urea} = 0.1$, 1.0, 10, and 100 mM. It is found that the solution in the hydrogel becomes more acidic as the concentration of urea $\overline{C}_{urea}$

16

increases, where a further increase of the concentration of urea $\overline{C}_{urea}$ (i.e. above 1.0mM) results in the pH gradient in the hydrogel. It has been reported in the open literature that the enzyme-induced pH gradient behavior has been employed in designing the biofuel cell, where the pH gradient is used to generate the potential difference in the biofuel cell system (Giroud et al., 2011). As such, the present urea-sensitive hydrogel is a promising material in the field of biofuel cell as it exhibits both the enzyme-induced pH and electrical potential gradients behavior, when subject to the urea concentration $\overline{C}_{urea}$ higher than 1000 mM, as seen in Fig. 5. Therefore, the urea-sensitive hydrogel could provide an innovative means for electricity generation from the human urine, which creates a new and affordable way of generating electrical power.

4. Conclusions

It is found that the urea-sensitive hydrogel is a promising material in the field of biofuel-cell as it exhibits both the enzyme-induced pH and electrical potential gradients behaviors in response to the urea, where it could provide a means for electricity generation from human urine. In future work, the MECurea model can be utilized to get a greater insight into the fundamental mechanism of the hydrogel in response to the urea cue.

Acknowledgement

References

Bae, Y.H., Okano, T., Kim, S.W., 1990. Temperature dependence of swelling of crosslinked poly (N, N alkyl substituted acrylamides) in water. Journal of Polymer Science Part B: Polymer Physics 28(6), 923-936.

Belytschko, T., Liu, W.K., Moran, B., Elkhodary, K., 2013. Nonlinear finite elements for continua and structures. John Wiley & Sons.

Blaedel, W., Kissel, T., 1975. Reactor-separator membrane combining immobilized urease and an anion exchange membrane. Analytical chemistry 47(9), 1602-1608.

Buron, C.C., Quinart, M., Vrlinic, T., Yunus, S., Glinel, K., Jonas, A.M., Lakard, B., 2014. Application of original assemblies of polyelectrolytes, urease and electrodeposited polyaniline as sensitive films of potentiometric urea biosensors. Electrochimica Acta 148, 53-61.

Chen, Chiu, 1999. Preparation and characterization of urease immobilized onto porous chitosan beads for urea hydrolysis. Bioprocess Engineering 21(4), 323-330.

Chen, Chiu, 2000. A poly (N-isopropylacrylamide-co-N-acryloxysuccinimide-co-2-hydroxyethyl methacrylate) composite hydrogel membrane for urease immobilization to enhance urea hydrolysis rate by temperature swing. Enzyme and microbial technology 26(5), 359-367.

Chen, Leu, Huang, 1994. Transport and hydrolysis of urea in a reactor–separator combining an anion exchange membrane and immobilized urease. Journal of Chemical Technology and Biotechnology 61(4), 351-357.

Chester, S.A., 2015. Gel Mechanics: A Thermo-mechanically Coupled Theory for Fluid Permeation in Elastomeric Materials. Procedia IUTAM 12, 10-19.

Chirizzi, D., Malitesta, C., 2011. Potentiometric urea biosensor based on urease immobilized by an electrosynthesized poly (o-phenylenediamine) film with buffering capability. Sensors and Actuators B: Chemical 157(1), 211-215.

Chowdhury, R., Bhattacharya, P., 1997. Mathematical analysis of unsteady-state dynamics of a liquid-membrane-encapsulated urease system. Industrial & engineering chemistry research 36(12), 5467-5473.

Deen, W.M., 1998. Analysis of Transport Phenomena, Topics in Chemical Engineering. Oxford University Press, New York.

Dezhong, L., Kai, G., Kang, C., Lihua, N., Shouzhuo, Y., 1996. Sensitive specialization analysis of urea in human blood by surface acoustic wave urea sensor system. Microchemical journal 53(1), 6-17.

Doi, M., 2013. Soft Matter Physics. Oxford University Press.

Drozdov, A., deClaville Christiansen, J., 2015a. Modeling the effects of pH and ionic strength on swelling of anionic polyelectrolyte gels. Modelling and Simulation in Materials Science and Engineering 23(5), 055005.

Drozdov, A., deClaville Christiansen, J., 2015b. Modeling the effects of pH and ionic strength on swelling of polyelectrolyte gels. The Journal of chemical physics 142(11), 114904.

Drozdov, A., deClaville Christiansen, J., 2015c. Swelling of pH-sensitive hydrogels. Physical Review E 91(2), 022305.

Duda, F.P., Souza, A.C., Fried, E., 2010. A theory for species migration in a finitely strained solid with application to polymer network swelling. Journal of the Mechanics and Physics of Solids 58(4), 515-529.

Eggenstein, C., Borchardt, M., Diekmann, C., Gründig, B., Dumschat, C., Cammann, K., Knoll, M., Spener, F., 1999. A disposable biosensor for urea determination in blood based on an ammonium-sensitive transducer. Biosensors and Bioelectronics 14(1), 33-41.

Ficalora, R.D., 2013. Mayo Clinic Internal Medicine Board Review. Oxford University Press.

Fidaleo, M., Lavecchia, R., 2003. Kinetic study of enzymatic urea hydrolysis in the pH range 4-9. Chemical and biochemical engineering quarterly 17(4), 311-318.

Fogler, H.S., 2010. Essentials of chemical reaction engineering. Pearson Education.

Giroud, F., Gondran, C., Gorgy, K., Pellissier, A., Lenouvel, F., Cinquin, P., Cosnier, S., 2011. A quinhydrone biofuel cell based on an enzyme-induced pH gradient. Journal of Power Sources 196(3), 1329-1332.

Grimshaw, P., Nussbaum, J., Grodzinsky, A., Yarmush, M., 1990. Kinetics of electrically and chemically induced swelling in polyelectrolyte gels. The Journal of Chemical Physics 93(6), 4462-4472.

Gurtin, M.E., Fried, E., Anand, L., 2010. The mechanics and thermodynamics of continua. Cambridge University Press.

Hamdy, S.M., El-Sigeny, S., Abou Taleb, M.F., 2008. Immobilization of urease on (HEMA/IA) hydrogel prepared by gamma radiation. Journal of Macromolecular Science, Part A 45(12), 980-987.

Hamilton, A., Breslin, C.B., 2014. The development of a novel urea sensor using polypyrrole. Electrochimica Acta 145, 19-26.

Hong, W., Zhao, X., Zhou, J., Suo, Z., 2008. A theory of coupled diffusion and large deformation in polymeric gels.

Illeperuma, W.R., Sun, J.-Y., Suo, Z., Vlassak, J.J., 2013. Force and stroke of a hydrogel actuator. Soft Matter 9(35), 8504-8511.

Jha, S.K., Topkar, A., D'Souza, S.F., 2008. Development of potentiometric urea biosensor based on urease immobilized in PVA–PAA composite matrix for estimation of blood urea nitrogen (BUN). Journal of biochemical and biophysical methods 70(6), 1145-1150.

Kovács, B., Nagy, G., Dombi, R., Tóth, K., 2003. Optical biosensor for urea with improved response time. Biosensors and Bioelectronics 18(2), 111-118.

Krajewska, B., Leszko, M., Zaborska, W., 1990. Urease immobilized on chitosan membrane: preparation and properties. Journal of chemical technology and biotechnology 48(3), 337-350.

Li, H., Luo, R., Birgersson, E., Lam, K.Y., 2009. A chemo-electro-mechanical model for simulation of responsive deformation of glucose-sensitive hydrogels with the effect of enzyme catalysis. Journal of the Mechanics and Physics of Solids 57(2), 369-382.

Liu, D., Chen, K., Ge, K., Nie, L., Yao, S., 1996. A new urea sensor based on combining the surface acoustic wave device with urease extracted from green soya bean and its application—determination of urea in human urine. Biosensors and Bioelectronics 11(4), 435-442.

Marchenko, S., Kucherenko, I., Hereshko, A., Panasiuk, I., Soldatkin, O., El'skaya, A., Soldatkin, A., 2015. Application of potentiometric biosensor based on recombinant urease for urea determination in blood serum and hemodialyzate. Sensors and Actuators B: Chemical 207, 981-986.

Marcombe, R., Cai, S., Hong, W., Zhao, X., Lapusta, Y., Suo, Z., 2010. A theory of constrained swelling of a pH-sensitive hydrogel. Soft Matter 6(4), 784-793.

Menichetti, L., Ortigoza, A.R., García, N., Giagnoni, L., Nannipieri, P., Renella, G., 2015. Thermal sensitivity of enzyme activity in tropical soils assessed by the Q10 and equilibrium model. Biology and Fertility of Soils 51(3), 299-310.

Miyata, T., Jikihara, A., Nakamae, K., 1997. Permeation decomposition of urea through asymmetrically urease immobilized ethylene vinyl alcohol copolymer membranes. Journal of applied polymer science 63(12), 1579-1588.

Moynihan, H., Lee, C., Clark, W., Wang, N.H., 1989. Urea hydrolysis by immobilized urease in a fixed bed reactor: Analysis and kinetic parameter estimation. Biotechnology and bioengineering 34(7), 951-963.

Nardinocchi, P., Pezzulla, M., Placidi, L., 2011. Thermodynamically based multiphysic modeling of ionic polymer metal composites. Journal of Intelligent Material Systems and Structures.

Novick, S.J., Dordick, J.S., 1998. Preparation of active and stable biocatalytic hydrogels for use in selective transformations. Chemistry of materials 10(4), 955-958.

Ogawa, K., Kokufuta, E., 2002. Enzymatic formation of pH gradients within polyelectrolyte gels with immobilized urease. Langmuir 18(15), 5661-5667.

Pandey, P., Upadhyay, S., Singh, G., Prakash, R., Srivastava, R., Seth, P., 2000. A New solid state pH sensor and its application in the construction of all solid state urea biosensor. Electroanalysis 12(7), 517-521.

Peterson, Eisenthal, R., Danson, M.J., Spence, A., Daniel, R.M., 2004. A new intrinsic thermal parameter for enzymes reveals true temperature optima. Journal of Biological Chemistry 279(20), 20717-20722.

Peterson, D., R, Danson, M., Eisenthal, R., 2007. The dependence of enzyme activity on temperature: determination and validation of parameters. Biochem. J 402, 331-337.

Plawsky, J.L., 2014. Transport phenomena fundamentals. CRC Press.

Teixeira, L.S.M., Feijen, J., van Blitterswijk, C.A., Dijkstra, P.J., Karperien, M., 2012. Enzyme-catalyzed crosslinkable hydrogels: emerging strategies for tissue engineering. Biomaterials 33(5), 1281-1290.

Thomas, R., Kanso, A., Sedor, J.R., 2008. Chronic kidney disease and its complications. Primary care: Clinics in office practice 35(2), 329-344.

Tijskens, L., Greiner, R., Biekman, E., Konietzny, U., 2001. Modeling the effect of temperature and pH on activity of enzymes: the case of phytases. Biotechnology and bioengineering 72(3), 323-330.

List of Table

Table. 1. Input data for the numerical simulation of the MECurea model.

List of Figures

Fig. 1. Schematic diagram of the urea-sensitive hydrogel system.

Fig. 2. Comparison of the equilibrium swelling ratio for the hydrogel between the simulation results by the MECurea model and Ogawa and Kokufuta's correlation, and their experimental data (Ogawa and Kokufuta, 2002) at initial radius $145.0\,\mu m$.

Fig. 3. The responsive swelling behavior of the hydrogel in response to the external stimulus of urea at different surrounding temperatures.

Fig. 4. The variation of the distributive profile of the electrical potential including the hydrogel and surrounding solution subject to different environmental urea concentrations.

Fig. 5. The distribution profile of pH of the gel and surrounding solution at 37 $^{\circ}$C.

Table 1. Input data for the numerical simulation of the MECurea model.

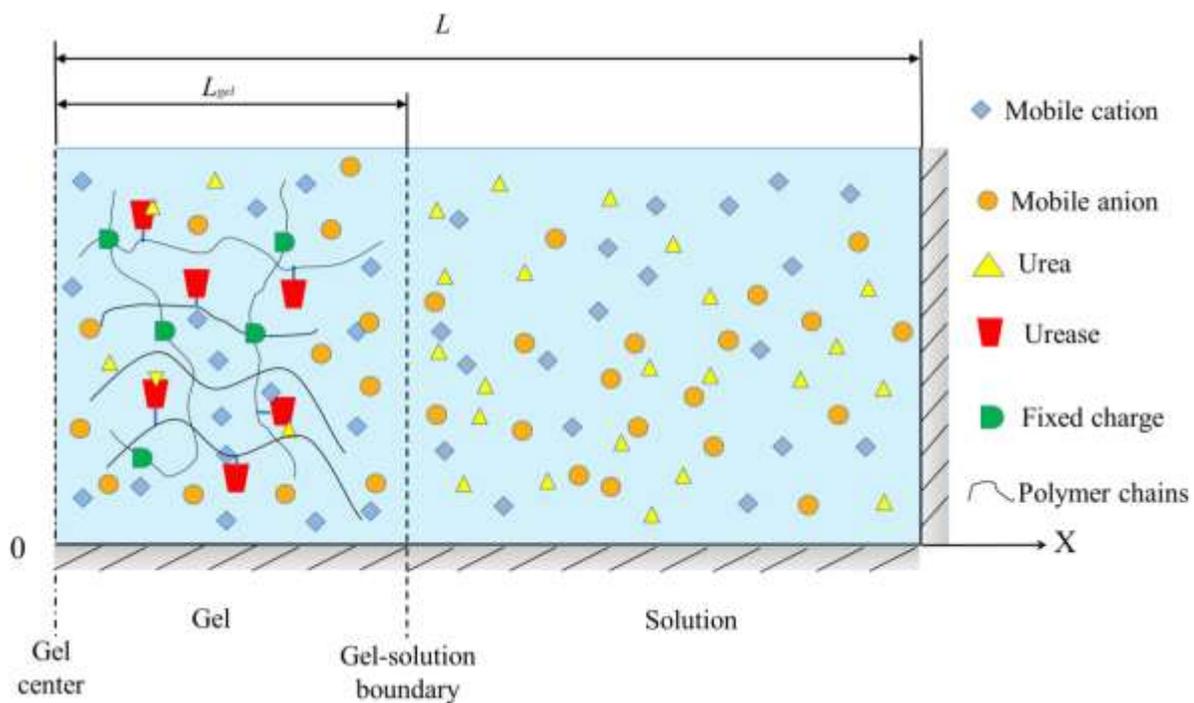| Parameter	Value
Diffusion coefficients D_{H^+} (Plawsky, 2014)	9.31x10^{-9} m^2/s
Diffusion coefficients D_{OH^-} (Plawsky, 2014)	5.24 x10^{-9} m^2/s
Diffusion coefficients $D_{NH_4^+}$ (Plawsky, 2014)	1.98 x10^{-9} m^2/s
Diffusion coefficients $D_{HCO_3^-}$ (Plawsky, 2014)	1.18 x10^{-9} m^2/s
Flory interaction parameter χ (Bae et al., 1990)	0.5090~0.9975
Permittivity $\varepsilon_r\varepsilon_0$ (water)	7.0832x10^{-10} A s/V.m
Michaelis constant K_M (Ogawa and Kokufuta, 2002)	2.82 mol/m^3
Reaction rate constant k_{cat} (Chen and Chiu, 1999)	1.5x10^3 1/s
Deactivation rate constant k_d (Chen and Chiu, 1999)	2.18x10^{-2} 1/s
Urease equilibrium temperature T_{eq} (Krajewska et al., 1990)	298.15 K
Urease optimum pH	7.4
Equilibrium constant K_W	10^{-14}
Equilibrium constant K_H (Fidaleo and Lavecchia, 2003)	7.57x10^{-4} mol/ m^3
Enthalpy change for transition from the active to inactive enzyme ΔH_{eq} (Chen and Chiu, 2000; Peterson et al., 2007)	89594 J/mol

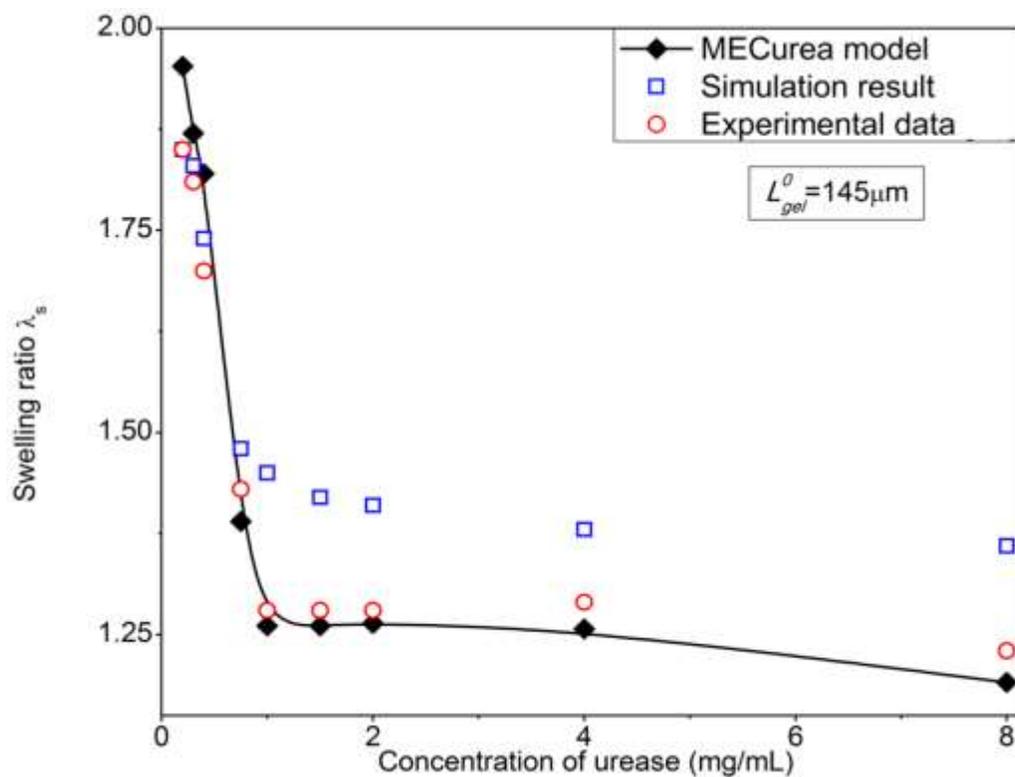**Fig. 1.** Schematic diagram of the urea-sensitive hydrogel system.

Fig. 2. Comparison of the equilibrium swelling ratio for the hydrogel between the simulation results by the MECurea model and Ogawa and Kokufuta's correlation, and their experimental data (Ogawa and Kokufuta, 2002) at initial radius $145.0\,\mu m$.
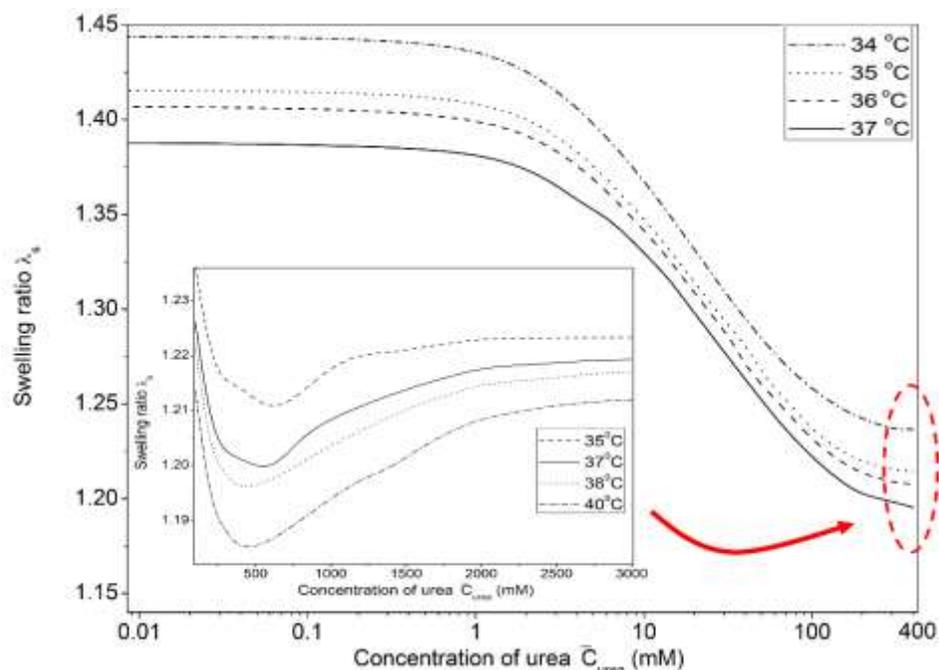
24

Fig. 3. The responsive swelling behavior of the hydrogel in response to the external stimulus of urea at different surrounding temperatures.
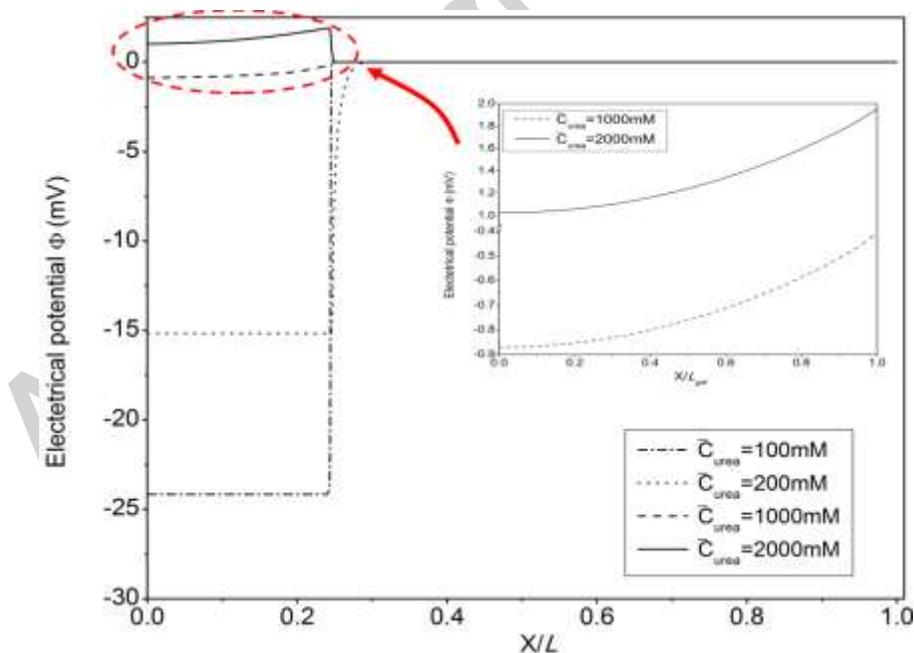

Fig. 4. The variation of the distributive profile of the electrical potential including the hydrogel and surrounding solution subject to different environmental urea concentrations.
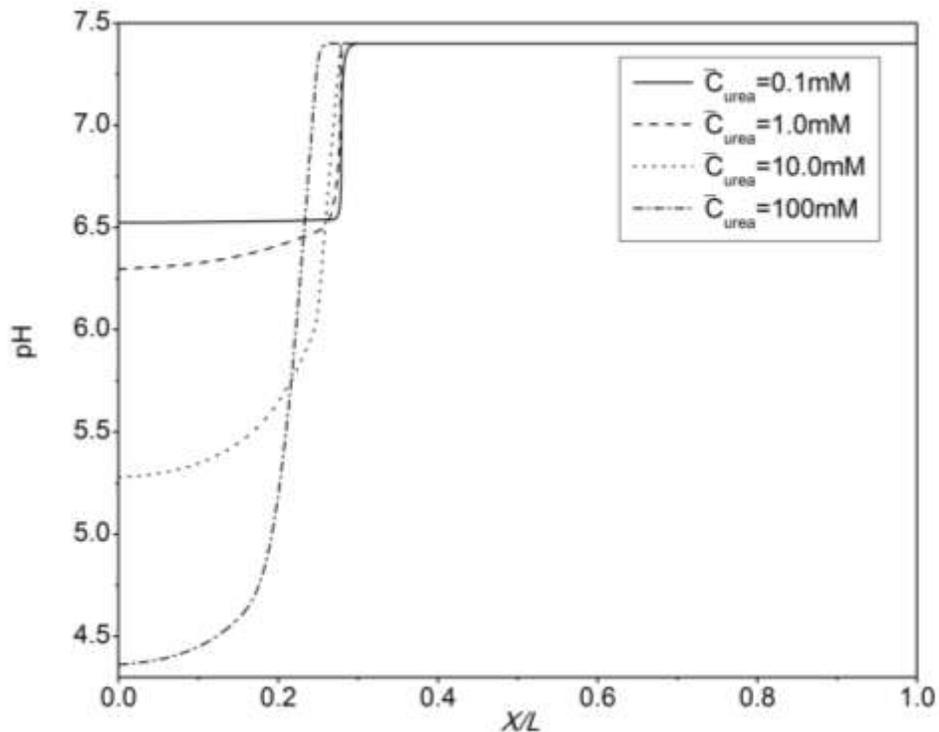
25

Fig. 5. The distribution profile of pH of the gel and surrounding solution at 37 $^{\circ}$C.

Highlights

- A 3D model has been developed to characterize urea-sensitive hydrogel as biosensor.

- The model couples the effects of biochemical, electro and mechanical together.

- The electrical, chemical and mechanical performances of the hydrogel are investigated.

- The hydrogel may generate electricity via the enzyme-induced pH and electrical potential gradients.